João Francisco Chibeles Rebelo Pestana Baptista

Developing assays to assess structure and function of synapses *in vitro*

Dissertação de Mestrado em Biologia Celular e Molecular, orientada pelo Doutor Alfredo Cabrera-Socorro (Janssen Pharmaceutica) e pela Professora Doutora Ana Luísa Carvalho (Universidade de Coimbra) e apresentada ao Departamento de Ciências da Vida da Universidade de Coimbra

Julho de 2016

UNIVERSIDADE DE COIMBRA

The work presented in this thesis resulted from a partnership between the University of Coimbra and Janssen Pharmaceutica NV, Beerse I. All experimental activities were performed at Janssen Pharmaceutica NV, Beerse I, a Johnson & Johnson pharmaceutical research and development facility in Beerse, Belgium.

Beerse, 2016

Acknowledgments

First, I would like to thank Dr. Alfredo Cabrera-Socorro for all his patience and precious lessons during the entire year. It was a true pleasure to be able to work in this project with you, where you taught me innumerous important lessons that I will never forget and will make use of them in the future.

To Dr. Andreas Ebneth for the great opportunity given to work in his group during this year, always in a fantastic working environment where we could share ideas and learn things. To all the department members whom I regularly contacted that helped me in the lab and for their patience and wisdom.

To my housemates and friends Rafaela Policarpo and Luís Gomes for rowing the same boat as me across this journey of great moments and for always being supportive. It was a short adventure that I wish it could continue for longer. Sometimes life was hard but with you it made it easier and memorable. Thank you!

To the fantastic Portuguese community at Janssen, Sara Calafate, Alberto Soares and André Marreiro which was a pleasure to meet and to share some good times together. To all the British and French students which I had the pleasure to befriend.

To all my friends in Coimbra in particular David, Luís, Carolina, Sara, Rui, for putting up with my weirdest ideas. To my colleagues and friends abroad in particular Nânci Winke for walking down the same road which is easier when it is shared.

Por fim, queria agradecer à minha família. Ao meu pai Luís de Pina e mãe Ticha por todo o apoio incondicional dado ao longo deste ano. Apesar desta curta mas longa estadia, senti-me sempre a um clique de distância de casa. Aos meus irmãos que apesarem de serem chatos a maioria do tempo, sem eles tudo teria sido diferente.

Abstract

There is no current treatment for AD. Historically, the access to human tissue has been a limitation for understanding of the pathogenesis of neurodegenerative diseases. Together with the lack of relevant in vitro models reproducing human neurophysiology, both factors have hampered the development of new therapies to treat neurological diseases. Recently developed stem cell technologies provide virtually unlimited access to human material. By transient overexpression of a set of transcription factors, somatic cells can be reprogramed into induced pluripotent stem cells (iPSCs) showing «stem cell-like» properties. iPSCs can be directly generated from patients and differentiated into any cell type of interest by using chemically and physically defined culture conditions.

Synapse loss is the strongest correlate of cognitive decline. iPSC-derived cortical neurons have been already validated for modelling neuropsychiatric disorders including autism, schizophrenia and neurodegeneration. However, a robust and scalable in vitro model of to assess synaptic function using iPSC doesn't yet exist. In this project we propose an in vitro model based on iPSC-derived cortical neurons co-cultured with astrocytes as a further step towards modelling synaptogenesis and synaptic degeneration. For this proof of concept study, we adapted already published protocols working in primary cultures and cell lines. We describe the combination of the classical dual SMAD inhibition differentiation protocol with Matrigel as embedding material for establishing a more robust and disease relevant model to assess synaptic structure and function. We used high-content imaging platforms combined with novel script analyses to quantify synapses in neuronal cultures, and monitored neuronal activity using multi-electrode arrays technology. We have developed a highly reproducible and optimally assay that works in several iPSC lines, providing a robust tool for supporting biomedical research and drug development in AD

Resumo

Não há tratamento actual para a doença de Alzheimer (DA). Historicamente o acesso a tecido humano tem limitado o entendimento da patogénese de doenças neurodegenerativas. Em conjunto com a falta de relevância dos modelos in vitro que reproduzem a neurofisiologia humana, ambos factores têm impedido o desenvolvimento de novas terapias para o tratamento de doenças neurológicas. Tecnologias recentemente desenvolvidas com células estaminais fornecem acesso virtualmente ilimitado a material humano. Através de sobrexpressão de um conjunto de factores de transcrição, células somáticas podem ser reprogramadas em células estaminais pluripotentes induzidas (iPSC em inglês) que possuem propriedades semelhantes às células estaminais. iPSC podem ser directamente geradas de pacientes e diferenciadas em qualquer tipo celular de interesse através de condições de cultura quimicamente e fisicamente definidas.

Neurónios corticais derivados de iPSC tem sido validados com o intuito de modelar distúrbios psiquiátricos como autimo, esquizofrenia e neurodegeneração. Contudo, ainda não existe um modelo robusto e escalável que permita análise de função sináptica usando iPSC *in vitro*. Neste projecto propomos um modelo baseado em neurónios corticais derivados de iPSC em co-cultura com astrócitos como uma nova medida no sentido de modelar sinaptogénese e degeneração sináptica. Como prova de conceito, adaptámos protocolos já testados em culturas primárias e linhas celulares. Descrevemos aqui um protocolo de diferenciação com inibidores SMAD com uso de matrigel como substracto para o estabelecimento de um modelo mais robusto e relevante para estudar a estrutura e função das sinapses em estado de doença. Usámos uma plataforma de imagem de alto desempenho em conjunto com um script para efectuar quantificação sináptica e monotorizámos actividade neuronal usando placas de multieléctrodos. Este método é altamente reproduzível e funciona optimamente em diversas linhas de iPSC comercialmente disponíveis, provando ser uma ferramenta robusta para uso em investigação biomédica e desenvolvimento de fármacos em DA.

Abbreviations

AD	Alzheimer's disease
APOE	Apolipoprotein E
APP	Amyloid precursor protein
ASB9	Ankyrin Repeat And SOCS Box Containing 9
BACE1	Beta-site APP-cleaving enzyme 1
BDNF	Brain derived neurotrophic factor
$CaCl_2$	Calcium chloride
cAMP	Cyclic adenosine monophosphate
CSF	Cerebrospinal fluid
DIV	Days *in vitro*
EOAD	Early onset Alzheimer's disease
EphB2	Eph tyrosine kinase B2
ER	Endoplasmatic reticulum
FAD	Familial Alzheimer's disease
FGF2	Fibroblast growth factor 2
GDNF	Glial cell-derived neurotrophic factor
GSK3β	Glycogen synthase kinase 3 bet a
HBSS	Hank's balanced salt solution
HCL	Hydrochloric acid
HEBS	HEPEs-buffered saline solution
HEPES	4-(2-hydroxyethyl)-1- piperazineethanesulfonic acid
ICM	Inner cell mass
iPSC	Induced pluripotent stem cell
LB	Lysogeny broth

LOAD	Late onset Alzheimer's disease
MAP	Microtubule-associated protein
MEA	Multielectrode array
MEM	Minumun essential media
MG	Matrigel
mGluR1	Metabotropic glutamate receptor 1
MS	Multiple sclerosis
MW	Multiwell
NFT	Neurofibrillary tangles
NMDAR	N-methyl-D-aspartate receptor
NPC	Neural progenitor cells
PBS	Phosphate-buffered saline
PBST	Phosphate-buffered saline with 0.25% Triton-X100
PD	Parkinson's disease
PDPK	Proline-directed protein kinase
PEI	Polyethylenimine
PET	Positron emission tomography
PLO	Poly-L-Ornithine
PrPc	Prion protein c
PSD95	Postsynaptic density protein 95
PSEN	Presenilin protein
SAD	Sporadic Alzheimer's disease
TE	Tris-EDTA
TrKB	Tyrosine Kinase Receptor B

Table of Contents

1 Introduction

1.1 Alzheimer's disease, prevalence and epidemiology

Alzheimer's disease is the most common form of dementia, a brain disorder that affects memory and cognitive functions resulting in decline in health and lifestyle in affected patients. This cognitive impairment affects nowadays 46 million people worldwide, a number that tends to triple by 2050. It has a great economic impact reflected by the high costs of the medical treatments and social care required by the patients. AD accounts for more than 70% of the total cases of dementia worldwide, most commonly seen in elderly people over 65 years. Depending on the age of onset, it can be classified as late onset or familial Alzheimer's disease (LOAD and FAD, respectively). FAD can also affect younger people therefore being called early onset or sporadic Alzheimer's disease (EOAD/SAD)[1]. Although memory loss and cognitive impairment are observed in both groups, different causes are thought to induce these symptoms in different onset periods. The FAD group, comprising only about 5% of the total population with the disease, presents faster disease progression mainly due to specific gene mutations. In the remaining group the symptoms do not seem to have a predominant genetic influence but rather a combination of genetic factors, changes in lifestyle and other risk factors. Interestingly, monogenetic forms of fAD can be used as a reductionist approach to model neurodegeneration *in vivo* and *in vitro*.

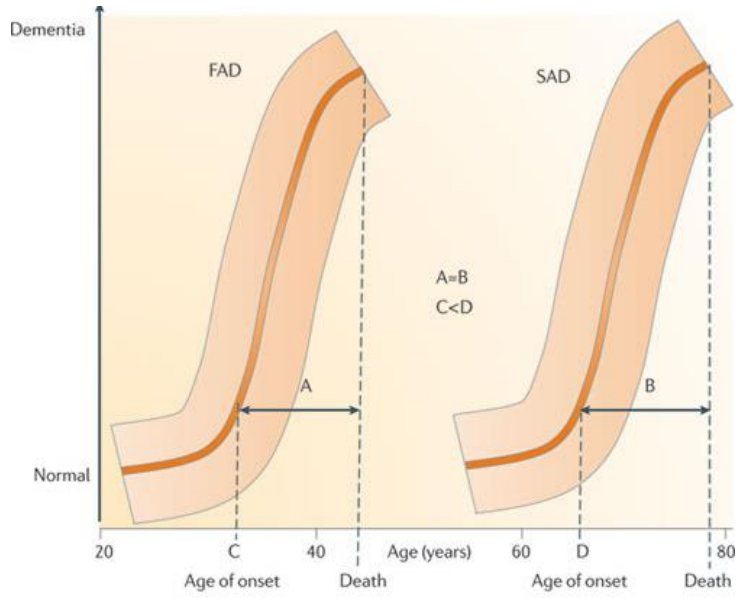

Figure 1. Age of onset of FAD and sporadic Alzheimer's disease individuals (SAD). Genetic mutations are thought to contribute to an early onset of AD with development of physiological and cognitive deficits. Individuals with SAD develop the symptoms in a later stage of their lives. Modified from ref[2]

1.2 Pathophysiology and cognition

AD is mainly characterized by the presence of two hallmarks identified as extracellular deposits of amyloid beta into amyloid plaques and aggregation of hyperphosphorylated misfolded protein in intracellular neurofibrillary tangles (NFTs). The extracellular amyloid fibrils deposits were revealed as consisting of aggregated small peptides later called amyloid beta (Aβ)[3]. This small peptide is produced by proteolysis of the single-pass transmembrane protein amyloid precursor protein (APP) cleaved by a family of enzymes that include α, β and γ-secretases. Depending on which enzymes are present, APP can follow an amyloidogenic or non-amyloidogenic pathway. In the non amyloidogenic pathway, the APP extracellular domain is cleaved by the α-secretase and the fragment APPs-α is released to the extracellular space. The remaining fragment termed C83 is retained in the membrane, where it is further cleaved by γ-secretase complex into a fragment P3 and the intracellular fragment AICD[4,5]. On the other hand, in the amyloidogenic pathway, beta-site APP cleavage enzyme 1 (BACE1) replaces α-secretase to generate APPs-β and a longer membrane fragment C99. Then C99 is further processed by γ-secretase which includes presenilin 1 and 2 enzymes, originating the extracellular amyloid beta (Aβ) fragment. The amyloid beta fragment is composed by 40 residues (Aβ40) but a longer and more hydrophobic variant with 42 residues (Aβ 42) is also produced although in lower proportion[6].

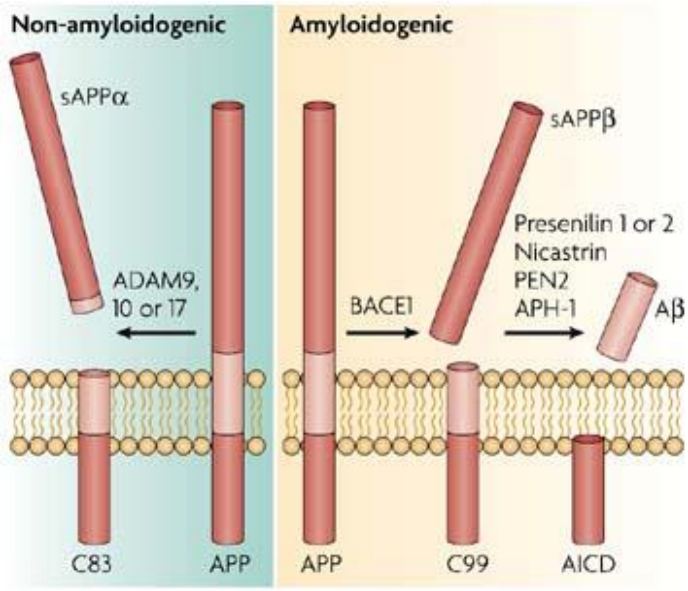

Figure 2. Generation of Amyloid-β peptide. Amyloid precursor protein (APP) can give origin to amyloid-β peptide following the non-amyloidogenic or amyloidogenic pathways when cleaved by different secretases. Modified from ref[7]

Neuronal growth and function is highly dependent on neurite transport of cellular machinery and molecules through the cytoskeleton. Microtubules and actin filaments are essential in this process. Microtubules are composed by tubulin monomers and allow the cell to maintain its structure. They also participate in the positioning of organelles such as mitochondria and other cellular and molecular machinery. One family of proteins that directly interact with the microtubules is the microtubule-associated protein (MAP) family which is comprised by the neuronal protein MAP2 alongside MAPT/tau and MAP4. In the brain tau is mostly expressed in the neuronal axons whereas MAP2 has higher expression in the cell body and dendrites[8] while MAP4 has ubiquitous expression. Tau gene spans over 110kbs and the alternative splicing of the primary transcript generates six different isoforms that that have different expression levels during the development of the brain[9]. Each isoform consists of an acidic projection domain and a microtubule binding domain which controls the rate of microtubule polymerization and the isoforms can be distinguished by the absence of one or two N inserts in the amino terminal and by the presence of either three (3R) or four repeat (4R) 18 amino acid long repeats in the carboxyl terminal of the protein. 4R tau forms, produced by alternative splicing and insertion of exon 10, have been described to aggregate faster than 3R forms[10] which might have implications in potential therapeutic interventions to treat AD.

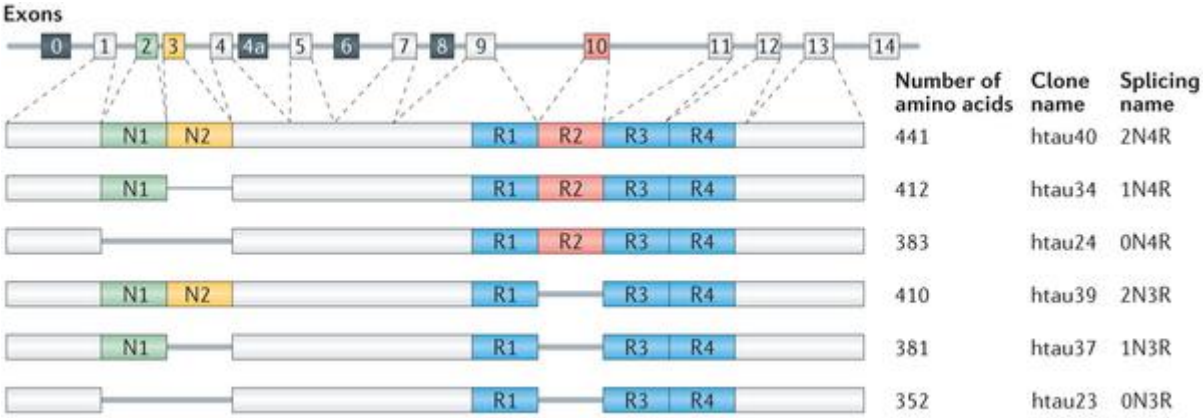

Figure 3. Human MAPT gene and the splice isoforms of tau. Six different tau isoforms are distinguished by the absence of one to two N inserts and by the presence of three to four 18 amino acid long repeats. Modified from Ref [11]

As any other protein, tau can undergo post translational modifications that modulate its function. One of the most important and common post-translational modification consists in the phosphorylation of specific residues which reduces its binding affinity to the microtubules and consequently the rate of polymerization. These modifications could have a strong impact in the event of irregular dysfunction during disease state. In general, these modifications are regulated

by kinases belonging to the groups of proline-directed protein kinases (PDPK), non PDPKs and tyrosine specific protein kinases[12]. SK3b is a kinase that contributes to phosphorilation of tau which was thought to be involved in tau aggregation in neurofibrillary tangles[13–15]. So it is expected than when tau protein is excessively phosphorilated it reduces microtubule polymerization and impairs axonal transport and that could explain the presence of intracellular fibrils observed before by Louis Alzheimer[16–18]. Other modifications described include glycosylation, glycation, propyl-isomerization, nitration, polyamination, ubiquitination, oxidation and truncation[19]. Tau can undergo truncation at both N and C terminals making it prone to aggregation into paired helical filaments (PHFs) and later promoting NFTs[20–22].

1.3 Disease mechanisms behind AD

Different hypothesis have been raised in an attempt to explain the genesis of the pathophysiological features seen in Alzheimer's disease. As stated previously, people with early onset AD have the disease due to genetic mutations usually in the APP gene as well as in the y secretase enzymes presenilin 1 and 2 genes[23,24]. Since in a healthy tissue a balance between production and clearance of any molecule is critical for a healthy cellular function, mutations in these proteins will affect the production rate of Aβ42/Aβ40 resulting frequently in the accumulation of the amyloid peptide monomers.

In the sporadic or late onset AD, the apolipoprotein E (APOE4) has been identified as the greatest genetic risk factor for late-onset AD. In the brain APOE is mainly produced by astrocytes and function as a carrier of cholesterol, aiding the transport and distribution of the lipid within and between neurons by binding to a low density lipoprotein receptor[25]. Three different isoforms (APOE2, APOE3 and APOE4) can be differentiated by different residues in the positions 112 and 158, which alter their conformation that affects their affinity to the respective receptors and other binding proteins such as amyloid beta [26]. When compared to the other isoforms, APOE4 possess a higher degradation rate and therefore decreases the availability of the carrier for cholesterol and amyloid beta clearance which may contribute for aggregation and deposition of plaques and further neurotoxicity and degeneration[27–29]. However, only 36% of the patients with Alzheimer's disease possess the allele coding for this particular isoform, suggesting that other factors may be contributing to the changes in the Aβ42 levels observed in the remaining fraction of patients.

Evidence suggests that tau also mediates some of the effects caused by amyloid beta. It was previously reported that incubation of rat cholinergic neurons with a highly toxic Aβ peptide

(Aβ25-35) resulted in the activation of MAPK and GSK3b kinases previously shown to be related to phosphorylation of tau[30]. Other studies showed a correlation between the low levels of Aβ42 with increased levels of phosphorylated tau in human CSF samples of aged subjects[31]. Because of its given function, abnormal dysfunction of tau may play an important role in the pathology of the disease, especially by impairing axonal transport of cellular cargo like mitochondria and other molecules to the synapses. Despite the link of tau with many different biological processes, the link between tau and neurodegeneration is proposed to be through its secondary effects as an aggregated protein within the cells by triggering cellular stress.

Neuropathological changes in AD precede the onset of cognitive symptoms[32]. Indeed, tau-pathology is already evident in brain sections of young people[33] (and is followed by the occurrence of amyloid pathology; Aβ-species are detectable in CSF as well as plaque pathology in brain visualized by PET imaging well before CSF-tau can be detected. Conceptually there is ample evidence that both amyloid- and tau-pathology are interdependent with Aβ-species accelerating tau-pathology by as yet unidentified mechanisms[34].

The theory that Tau pathology is spread in a prion-like process of template conformational change emerged in the last few years. It is supposed that misfolded Tau species act as seeds which recruit other Tau proteins into pathological aggregates[35]. Hence, seeds are more and more considered as aggregation triggers which are able to expend in the brain following a cell to cell propagation fashion, thus facilitating the spread of Tau pathology. Following this theory, Guo and Lee from Philadelphia presented a neuronal model in which synthetic tau fibrils made from recombinant protein trigger the Tau aggregation, forming neurofibrillary tangle-like insoluble aggregates in mouse primary hippocampal neurons over-expressing human tau[36]. The properties of the fibrils provide seemingly a very efficient Tau aggregation triggering in the neurodegenerative models used in the therapeutic drug discovery field.

1.4 Mechanisms behind tau and synaptic dysfunction

At the post synaptic level, tau seems to interact with the tyrosine kinase Fyn which in turn participate in the phosphorylation of NMDA-R and its anchorage to the membrane by the post synaptic density protein PSD-95[37]. This anchorage may have two direct consequences, by enhancing the activation of downstream pathways or mediating toxicity effects caused by protein-ligand interactions. In P301S animal retinal cells, a decrease in BDNF protein levels and TrkB receptor upregulation was found however, TrkB was uncoupled from the downstream effectors, reinforcing the important role of tau in the modulation of receptors activity[38]. It has also been shown that direct binding of Aβ oligomers to a subunit of NMDA receptors induced oxidative stress seen by increased ROS production probably involving mitochondrial dysfunction[39]. Other receptors have been also proposed to play a role in amyloid beta mediated toxicity like mGluR5, acetylcholine receptors, EphB2, PrPc however it is not clear yet how Aβ and tau mediate toxic responses through these receptors[40]. Tau ablation in mouse primary neuronal cultures shown to decrease amyloid-mediated GSK3b activation to basal levels and mitochondria recover their movement rate which was dependent on that kinase. Moreover, tau truncation of the C-terminal containing the microtubule binding domain does not reduce axonal transport deficits caused by amyloid beta neither it does require interaction with Fyn kinase suggesting that tau may mediate amyloid beta toxic function at the post synaptic level in a microtubule independent way[41]. Besides its role at the post-synaptic compartment, tau is also released from the presynaptic compartment by mechanisms that still to be elucidated.[42]

So far most of these studies have looked at molecular and cellular changes in murine cellular and animal models presenting genetic mutations in amyloid beta related proteins APP, PSEN1/2 and in tau. One major limitation is that these models have been focused in single aspects of the disease and do not recapitulate all the aspects that an AD human brain would have. Nevertheless, they are very important to help shed light in some of the mechanisms that may be underlying neuronal synapse loss of structure and function. An ideal model would have to mimic the human aspects of the disease and therefore that could be used in translational medicine to study the pathophysiological mechanisms and development of new effective drugs. One breakthrough in this direction was the discovery of cellular reprogramming which in theory would allow to create human cells in vitro.

As explained before, hyperphosphorylated tau and amyloid beta toxic forms will disrupt the healthy synaptic structure and function. Synapse loss has been observed as the strongest

quantitative pathological attribute that correlated with cognitive deficits in biopsies and autopsies of individuals with AD after subjected to different cognitive tests[43–45].

Moreover, reduction in the synapse numbers was associated with decrease in post and presynaptic protein levels such as synapsin, synaptophysin and PSD-95 seen in different cortical regions of patients with AD [45] or mild cognitive impairment[46] . This suggests that disruption of the physiological synaptic mechanisms may precede synapse loss in the very early stages where the cognitive defects are not severe enough to affect the daily activities of the patients. Taking in consideration that the pathophysiological aspects of the disease are complex and intricate, trying to modulate them in a single representative model is difficult to achieve.

1.5 Pluripotent Stem cells

All mammal embryos result from the fertilization of the egg by the sperm resulting in a single cell called zygote. This cell then starts to divide giving rise to a structure called morula and after a number of divisions a cavity inside the globular structure forms creating the blastocyst. The cells in the inner cell mass of the blastocyst possess a particular characteristic of being able to generate every cell types from the three embryonic germ layers (endoderm, mesoderm, and ectoderm) and to the germ lineage. During the remaining embryogenesis stages cells from these layers will contribute for the formation of the different tissues of the embryo. The first embryonic pluripotent stem cells were successfully isolated and cultured in 1981 by Evans and Kaufman from the ICM of mouse blastocysts and displayed similar behavior as tumural cells[47]. Because each adult human cell is derived from the cells present in the blastocyst, these pluripotent cells could be important to study different aspects of human cell differentiation and possibly the study of diseases. However, mainly due to ethical and availability problems, it turned extremely hard to use cells directly isolated from human embryos. To circumvent these restrictions a new way of obtaining human stem cells was needed. In a first attempt, transduction of primary mouse embryonic and adult fibroblasts with a specific set of transcription factors allowed them to obtain pluripotency and thus originating induced pluripotent stem cells. This process of transforming adult somatic cells into pluripotent cells was called cell reprogramming and was soon successfully applied to human fibroblasts with full potential to differentiate into cells from the different germ lines[48].

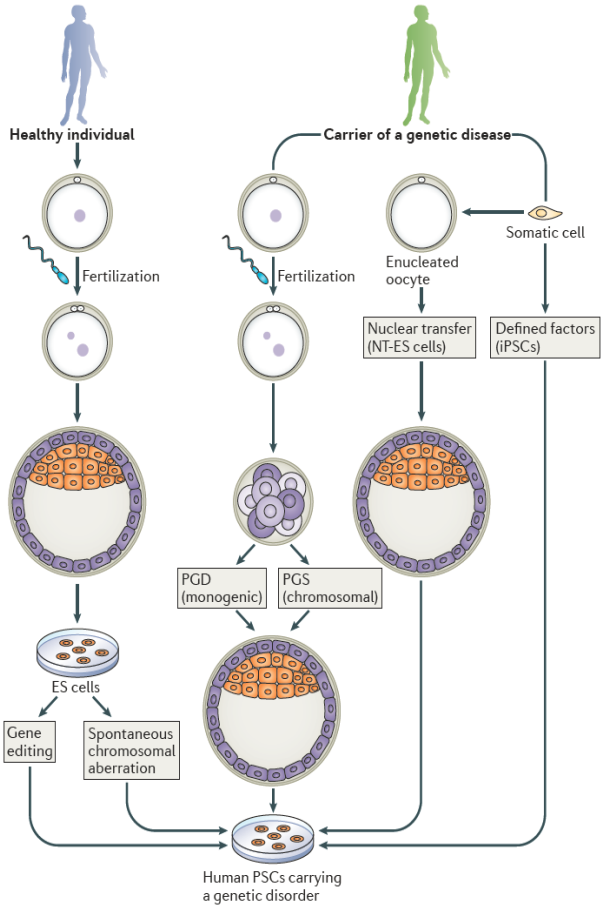

Figure 4. Generation of human pluripotent stem cells (PSCs) carrying genetic mutations from healthy and disease patients. Pluripotent stem cells can be generated from isolated embryonic stem cells from healthy or disease individuals or from somatic cells by the overexpression of specific transcription factors which are able to induce a state of pluripotency. These cells can be differentiated into lineage specific cell lines such as neuronal cell lines. Generation of a mutated cell line can be achieved by these methods either by gene editing or directly from disease individuals. Modified from Ref[49]

1.6 Human neurons to model neurodegeneration in vitro

1.6.1 APP models

In the first iPSC model reprogrammed primary fibroblasts from two patients with SAD and two subjects with FAD bearing duplication of the APP gene[50]. In all iPSC lines except one derived from a subject with SAD, there was an increase in the total amyloid protein levels, phosphorylated tau and activation of GSK3beta that were partially blocked by b secretase inhibitors but not y secretases. The distinct results between the two SAD iPSCs neuronal lines may result from genetic differences which difficult the use of sporadic derived neurons as a disease model.

In other studies, iPSC derived neurons with a recessive mutation APP E693Δ and V717L mutation of subjects presenting early onset symptoms but lacking deposition of amyloid plaques were differentiated into cortical neurons[51]. Intracellular levels of Aβ40 and Aβ42 in the E693Δ mutated neurons were not different from the control cells although it was observed accumulation of intracellular Aβ oligomers. As a consequence, there was an increase in the production of reactive oxygen species and increased levels of ER stress which were completed abolished when a beta secretase inhibitor was applied. In contrast, V717L mutated cells showed increased levels of amyloid beta 42 but no marked accumulation of oligomers [51]

Muratore also looked into the V717L mutated cells and observed similar changes in Aβ42 levels and noticed increases in total and phosphorylated tau levels that were blocked when cells in the early stages of differentiation were treated with antibodies against amyloid beta, supporting the idea that tau pathology is located downstream of Aβ[52] .

Other studies have used iPSC cells of subjects with mutations on the gene encoding presenilin 1 and 2. In one study, iPSCs derived from subjects with each one of these mutations showed noticeable increase Aβ42/Aβ40 ratio when compared with control cells. The cells were then treated with two different y-secretase inhibitors only one was able to decrease the ratio by depleting secretion of Aβ42 to the media[53] . Additionally it was found upregulation of NLRP2 gene which is involved in pro-inflammatory responses and ASB9 gene which codes a protein that targets for degradation a mitochondrial creatine kinase[54] . Since this kinase has an important role in providing ATP for the neurons, its degradation ultimately impairs mitochondrial function and may further enhance cellular degeneration. More recently Moore et al (2015) compared Aβ and tau protein levels between a duplicated app, presenilin 1 mutant model and app V117L model. As expected from previous papers, Aβ42 levels were higher in all mutants when compared with control cells. However increase in total and phosphorylated tau was not observed in the presenilin 1 mutant cells suggesting that Aβ42 alone is not capable of driving tau phosphorylation in this model [55].

In other study, immortalized human neural progenitor cell line from human fetal brain called ReN cells of transfected to express mutations in the APP, PSEN1 and a double APP/PSEN1 mutation to enhance amyloid beta toxicity[56]. The cells were differentiated in a three dimensional Matrigel culture system that could limit movement of the neurons and amyloid species produced. Accumulation of oligomeric amyloid species and phosphorylated tau was found in all cells including deposition of tau fibrils, features that were almost depleted by beta and gamma

secretase inhibitors, suggesting it may successfully recapitulates successfully Alzheimer's pathology.

1.6.2 TAU models

More recently, iPSC technology has been used to model familial forms of AD associated to mutations in MAPT gene. Splice mutations affecting exon 10 have been of special interest due the link between 4R forms of tau and the formation of intracellular aggregates[10]. Recent publications have suggested a direct correlation between the 4R forms of human tau and neuronal activity[57,58] . iPSC have been derived from patients carrying the intronic mutation N279K, which leads to an imbalance of the 3R:4R isoform ratio. When differentiated into cortical neurons these cells exhibit earlier electrophysiological maturation[57]. Similar results have been observed in a different model using mice in which human-tau 4R form is replacing endogenous tau. These human-Tau mice display enhanced seizure severity following pentylenetetrazole injection[58]. However, little is known about the role of Tau in synaptic function and only recently this has started to be addressed.

1.7 Objectives

Synaptic loss is found in patients with AD, Parkinson's disease (PD) and Multiple Sclerosis (MS) among other neurodegenerative disorders. Disease-relevant human models of to study synaptic structure and function are urgently needed for better understanding related pathologies and for the development of new treatments aiming either to stop synapse degeneration or promote neuronal connectivity. Current in vitro models, as primary cultures, lack the physiological relevance and compatibility with miniaturized formats needed to test large compound libraries. Human derived induced pluripotent stem cells (iPSCs) allow the generation of cortical neurons *in vitro* providing a more scalable and disease-relevant model. However, a major issue in modelling neurological diseases using stem cells is the lack of standard differentiation/maturation protocols that efficiently overcomes variability between laboratories or cell lines. Scalability, long term adherence, cell distribution or slow maturation are among the biggest issues when translating stem cell technology to the drug development pipeline. Under conventional coating conditions neurons are differentiated on plates pre-treated with a mixture of laminin and poly-lysine/poly-ornithine. Although this method has historically provided optimal results in primary cultures, it has been difficult to translate to human iPSC-derived cortical neurons in a scalable manner for long term cultures. Interaction between cells and coating material over the time affects integrity of adhesion molecules and ultimately drives to cell detachment. This problem can be solved by embedding cells in scaffolding bio-compatible materials enriched in adhesion molecules. Only recently, these biomaterials have started to be used as an alternative to the classical Poly-ornithine/Laminin based coating protocols[59]. Providing scaffold to differentiating neurons in vitro is a key property that could help to establish a robust and stable synaptic connectivity between cells. Importantly, synapse stability and strength is crucial for imaging and quantification in phenotypic studies (e.g. high content imaging, HCI). Embedding substrates as Matrigel (so called 3D cultures) allow passive diffusion of culture media, and provide extra additional stability against physical stress caused by media changing or plate handling. Matrigel® is a solubilized basement membrane preparation enriched in laminin, collagen IV and other extracellular matrix proteins. When differentiated in Matrigel®, hiPSCs generates a high yield and purity of forebrain cortical neurons[52]. The low batch-to-batch variability of Matrigel has been the most important property to support use in stem cell cultures provided its capacity to maintain pluripotency of ES and iPSCs. Based on its reduced batch-to-batch variability, it is reasonable to hypothesize that Matrigel® could also allow yield reproducibility and robustness to neuron based assays.

The current research project aims to establish a robust, scalable and disease-relevant *in vitro* model of synaptic connectivity to be used for drug screening in AD. The central hypothesis of this study is that differentiating cortical neurons using enriched embedding biomaterials and astrocytes can provide a physicochemical context that better mimics their natural environment in the nervous system. By providing such conditions, iPSC derived neurons can be maintained in culture for a longer time and used for high throughput/content assays modelling neurodegeneration.

Several parameters have been optimized to address proposed objectives. Our work with primary cultures was focused in the antibody validation and transfection protocols. We tested a battery of markers that were subsequently used for staining iPSC-derived neurons. The transfection protocols was also optimized to yield a higher transfection efficiency and was optimized for the reporters described. For the second phase, we optimized the protocol for differentiation and maturation of human cortical neurons. The classical dual SMAD inhibition protocol[60] was used as starting point and adapted afterwards to our experimental set up based on co-culture with murine astrocytes. Working dilution of Matrigel and number of cells per well were optimized to a 96-well plates and MEAs format in which identity, maturity and activity of neurons was checked by different approaches. Once the neuronal differentiation protocol was established, we designed the assay to detect neuronal activity using a multi-electrode array (MEA) platform (Axiogenesis). Time course analysis was performed in order to identify baseline values and optimal timing for pharmacology (defined by the time point at which the highest activity was detected). To finally confirm robustness of the assay, we reproduced our data using different culture conditions comparing classical laminin coating with Matrigel embedding. Overall, the set of assays described in this report allowed us to validate the optimal culture set up for modelling synaptogenesis and synaptic degeneration in vitro.

In conclusion, this research project has achieved the following major goals:

1. Development of an *immunofluorescence toolbox* and image analysis script for the assessment of synaptic pathology.
2. Design *High Content-compatible* fluorescence reporters to assess synaptic structure and function *in vitro*.
3. Development of a robust and reproducible standard operating procedure (SOP) to assess synaptic activity using human iPSC-derived cortical neurons.

2 Materials and Methods

2.1 Media

iPSC N2B27 medium is composed by Neurobasal Medium (Life Technologies) and DMEM/F-12 Glutamax (Life Technologies) supplemented with 1x B-27 supplement (Life Technologies), 1x N-2 supplement (Life Technologies), 2.5x Glutamax (Life Technologies), 2.5x MEM Non-Essential Amino Acids (Life Technologies), 0.5mM sodium pyruvate (Life Technologies), 10U/mL penicillin-streptomycin (Life Technologies), 50µM 2-mercaptoethanol (Life Technologies), 250µL insulin human solution (Sigma-Aldrich). *Differentiation medium* consisted of iPSC N2B27 medium supplemented with 1mM cAMP (Sigma-Aldrich), 20ng/mL BDNF (R&D Systems), 20ng/mL GDNF (R&D Systems) and 200µM ascorbic acid (Sigma-Aldrich). *Glial medium* used for astrocytic cultures is MEM (Life Technologies) supplemented with 50mL heat-inactivated horse serum (Life Technologies). *Primary culture medium* B27 L-Glutamine consists on neurobasal medium with 2x B-27 supplement and 5x Glutamax.

2.2 Human iPSC derived neuronal cultures

Induced pluripotent stem cell lines used were differentiated by Axol Biosciences: parental control (iPSC0028 Sigma-Aldrich), double mutant MAPT 7H6-A1. The double mutant expresses both an isogenic mutation on the intron 10 of tau/MAPT gene (Alzforum MAPT IVS10+16 C>T) and P301S mutation on the exon 10.

Neural progenitor cells (NPCs) with 30DIV were generated and prepared as frozen stocks by Axol Bioscience following described protocols. The vials were thawed at 37°C and media was added to dilute the DMSO. After 4min centrifugation at 300g the supernatant was removed and the cells suspended in N2B27 media supplemented with 20ng/mL FGF2. Then the cells were plated in 0.01% PLO/laminin pre coated 6 well plates (1hour coating with 0.01% Poly-L-ornithine, washed once with 1xPBS and 1h coating with 0.01% laminin). The day of thawing was considered as 0 days *in vitro*. Two days FGF2 was removed from media. On the third day the final plating takes place: cells are washed once in 1xPBS, incubated for 5-10min with accutase and slightly tapped until cell detachment is observed. Media was subsequently added to prevent accutase toxicity and cell density was determined with an automated cell counter. Cells in suspension were centrifuged at 300g for 5min and resuspended in a volume of media reaching a final density of one million cells per milliliter. Cells were either directly plated in PLO/Laminin coated wells or centrifuged and resuspended in diluted BD Matrigel in media solution, at a dilution of 1:10 for 96wp and 1:3 for coverslips. The NPCs were either seeded without astrocytes or in co-culture with mouse or human

astrocytes in a ratio of 1:1. The plates were left in the hood for 5-10 minutes until sedimentation in a single layer of cells was observed followed by 5-10 minutes incubation at 37°C to allow a final solidification. Afterwards, media was added to the plated wells and PBS around to prevent evaporation. On the day after subplating the media was replaced by media containing 10µM N-[N-(3,5-difluorophenacetyl)-L-alanyl]-S-phenylglycine t-butyl ester (DAPT), an inhibitor of the Notch signaling used to block cell proliferation[61]. The treatment was repeated after 48h and differentiation medium was added with half medium change every three days until sampling. Cells were plated at a density of 60000 cells per 48-well of MEAs plates, 30000 cells per 96-well.

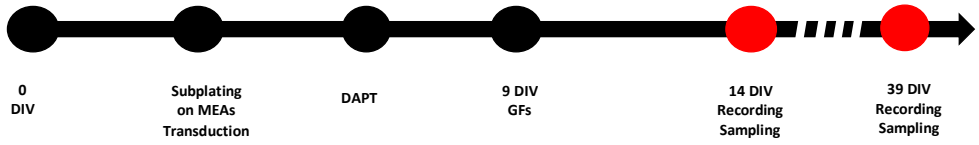

Figure 5. Scheme showing differentiation process starting from the frozen vial. Sampling time for electrical recordings and immunostaining are highlighted in red.

2.3 Astrocytic and primary neuronal cultures

E19 C57BL/6J pregnant mice was sacrifice and the brains removed from the embryos according to standard procedures. Astrocytic cultures were prepared following an adaptation of Kaesh et Banker 2006 culture protocol[62]. The brains were dissected and kept in Hibernate (Sigma-Aldrich) or HBSS dissection medium. The cerebellum and olfactory bulbs were removed and the meninges were carefully striped from the brain. The remaining tissue which included cortex, hippocampus and striatum was transferred to a sterile falcon tube where was washed three times with glial medium. On the last wash, the brain tissue was transferred to a new tube where was dissociated 100x with a flamed Pasteur pipette with a reduction of the lumen diameter to half of the initial dimension. The dissociation was further enhanced by using a flamed Pasteur pipette with smaller lumen. The dissociated cells were then seeded on 75cm^2 culture flasks. On the following day, the flasks were vigorously tapped to allow the detachment of non-astrocytic cells and debris and to reduce toxicity caused by the release of cytokines during and after the tissue dissociation. Fresh medium was added and the astrocytes were kept in culture with half media changes every three days, until seeded with human neurons.

Wistar WT rats at gestational day E18-19 were used for primary neuronal cultures, a procedure done by Sofie Versweyveld. The cortices were manually removed and transferred to pre-warmed

HBSS/HEPES buffer (7mM HEPES, 100U/mL Penicillin-Streptomycin). After the cortices have been dissected, they were chemically dissociated by trypsinization (0.05% trypsin in HBSS/HEPES buffer) during 15 minutes at 37°C. In the end of the incubation, the brain tissue was washed three times with MEM-horse to block the trypsin proteolytic activity. Mechanical dissociation was done by pipetting 15-20 times with two flamed Pasteur pipettes with normal and half size tip diameter. Cell density was calculated and the suspension was centrifuged at 1000rpm for 5 minutes. The cells was resuspended in MEM-Horse medium and were plated at the desired density in the MW plate. After acceptable cell attachment was observed, the plating medium was replaced by primary culture medium, with fresh medium change once every week.

2.4 Gene constructs, DNA amplification and purification

All constructs used in this project were synthesized by Genewiz Co upon request. One shot TOP10 chemically competent *E. coli* bacteria were thawed and 1µL of the plasmid DNA in need was added at a concentration of 100pg/µL. To prevent mechanical stress of the bacteria, the vial was gently tapped and then incubated on ice for 30 minutes. Afterwards, the cells were heatshocked for 30 seconds at 42°C water bath and placed on ice for 2 minutes. 250µL of pre warmed SOC media was added and the vials were incubated horizontally for 1 hour at 37°C and 225rpm in a shaking incubator. 100µL of the transformed cells were spread on LB agar petri dishes containing the appropriate antibiotic and incubated overnight at 37°C. On the following day, single colonies were picked and incubated in 5mL of LB media with respective antibiotic for 8 hours until significant growth was observed. The bacteria liquid culture was further amplified by mixing 1mL of the previous solution with 110mL of fresh LB media with respective antibiotic and kept incubating overnight. DNA was purified from the liquid bacteria cultures by using either the Qiagen HiSpeed® Plasmid kits (Qiagen) or PureLink® HiPure Plasmid Kit (Invitrogen).

2.5 Calcium phosphate transient transfection

Primary neuronal cultures and iPSC derived neuronal cultures were transfected using a calcium phosphate transient transfection protocol. First, 1µg of the DNA to be transfected into the cells was mixed with TE buffer or sterile water and 0.25M of $CaCl_2$ was added dropwise, with a gentle vortex afterwards. The DNA-Calcium phosphate precipitate was prepared by pipetting the TE/DNA/$CaCl_2$ in a dropwise mode to an equal volume of 2xHEPES buffered saline solution (HEBS) and incubated for 30minutes in the dark with 5-10 seconds vortex every 5 minutes. Half of the conditioned media was removed from the wells and 2mM kynurenic acid (Sigma-Aldrich) diluted

in non-conditioned media was added. In the end of the precipitate formation, 25µL of precipitate was added dropwise to each well and cells were incubated for 2h at 37°C. Formation and distribution of the precipitates was tracked after one hour of incubation period. After incubation, the transfection media containing the precipitates was removed and the precipitates were dissolved with an acidic solution composed by 2mM kynurenic acid and 3mM HCl diluted in media for 17minutes at 37°C. The cells were then washed once and half conditioned medium was added back with addition of fresh medium.

2.6 Immunocytochemistry

Neurons were fixed in 4% paraformaldehyde, 4% sucrose in PBS for 10 minutes, washed three times in PBS. Cells were then permeabilized for 10 minutes in 0.25% Triton X-100 in PBS (PBST) followed blocking in 1%BSA in PBST. Incubation with primary antibodies was done either at RT for 1 hour or overnight at 4C and washed afterwards with PBST. Cells were then incubated with secondary antibody for 1 hour at RT, washed three times with PBST, counterstaining for 4min with DAPI and washed with PBS. For AMPAR staining, incubation with primary antibody was performed overnight in non-permeabilizing conditions, after blocking with 1%BSA/PBS. After antibody removal and washings, the staining of the intracellular proteins was done as described above. The primary antibodies used included chicken anti-MAP2 (1:200; Aves Lab), mouse anti-PSD95 (1:200; Abcam), mouse anti-Huc/D (1:50; Sigma-Aldrich), mouse anti-Synapsin (1:500; Synaptic Systems), phalloidin conjugated secondary antibody (Thermo Fisher), rabbit anti-TUJ1 (1:500; Abcam), mouse anti-Tau (1:11000; DAKO), rabbit anti-Vglut1 (1:1000, Synaptic Systems), guinea pig anti-synaptophysin (1:1000; Synaptic Systems), mouse anti-GFAP (1:1000; Millipore), rabbit anti-tRFP (1:1000; Evrogen). Images were acquired with LSM510 laser confocal microscope (Carl Zeiss) or with Opera Phenix High Content Screening System. Images were processed with Harmony High-Content Imaging and Analysis Software or ImageJ and Columbus Image Data Storage and Analysis System image software from Perkin Elmer was used to analyze the synaptic markers colocalization with an in house developed script. The script performs batch analysis of stack images acquired with the Phenix microscope, with identification of synapses on a mask drawn around the neurites.

2.7 Multi-well MEA plates recordings and data analysis

Microelectrode array plates were composed by 48 wells with each well containing 16 nano-textured gold electrodes with 40-50µm diameter spaced 350µm center-to-center (Axion Biosystems). Prior to cell plating, each well was coated with 0.1% PEI solution and incubated for at

least 30 minutes at 37°C. After removal of the PEI solution, the wells were extensively washed with sterile water and left drying overnight under the hood. Cells were directly plated at a density of 60000 cells per well in pre-coated 0.01% laminin MEAs plates or diluted Matrigel in 1:10 N2B27 medium. Half change of medium was performed 4 to 24 hours prior recording. Spontaneous activity from iPSC derived neuronal cultures between 44 and 69DIV was recorded using the Maestro Axion's 768 channel system with Axion Integrated Studio 2.3 software at 37°C and 5% CO_2. An active electrode was considered when it detected more than 5 spikes per minute and data was analyzed when at least 15% of the electrodes were active. Different parameters were calculated including the number of spikes and number of bursts which were considered as groups of at least 5 spikes spaced at least 100ms apart. The mean number of spikes fired per second or mean firing rate was also calculated with the respective standard deviation of the average value of all active electrodes

3 Results

3.1 Differentiation of hiPSC into neurons and cultures characterization

NPCs were differentiated over a period that exceeded four weeks following already published protocols. The majority of the cells were positive for the neuronal markers HUC/D and MAP2 which also presented cortical identity by expressing CTIP2 and TBR1 (Figure 6A). In order to enhance neuronal maturation we have co-cultured iPSC derived cortical neurons with mouse astrocytes. We have performed immunostaining at 32-35DIV with antibodies against synaptic proteins PSD-95, synaptophysin and AMPA-R alongside the neuronal marker MAP2 (Figure 6B-C). We observed neurite staining with MAP2 however, it was also observed inside additional structures (Figure 6B). Furthermore, PSD-95 and AMPA-R proteins were identified in the same structures, which could indicate protein expression on the astrocytes in culture. Synaptophysin was the only marker that seemed to be expressed exclusively on the neurons (Figure 6B-C).

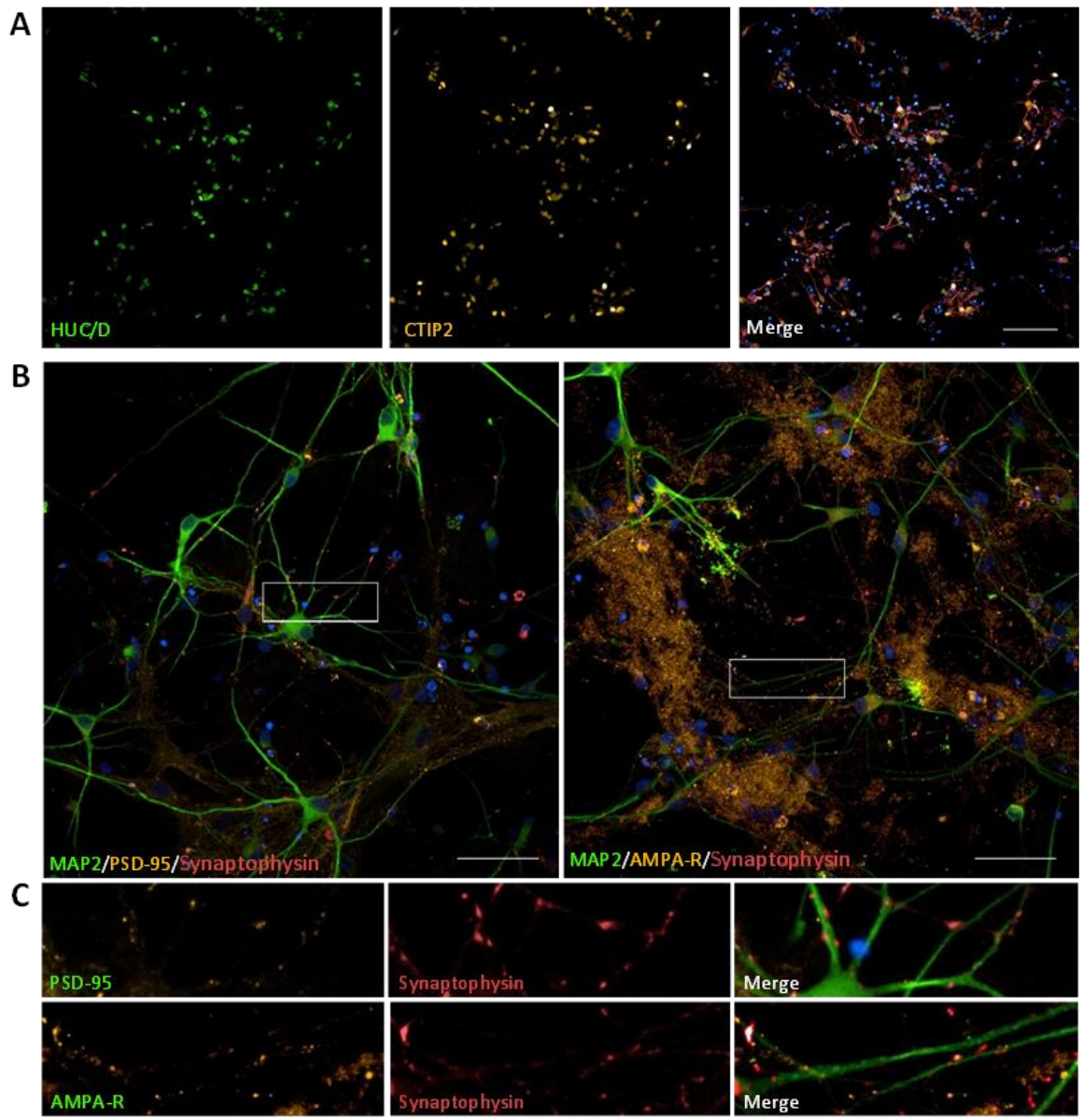

Figure 6. iPSC derived neuronal cultures characterization (A) Confocal analysis of parental control iPSC derived neurons co-cultured with mouse astrocytes at 3DIV and fixed at 30DIV immunostained for HUC/D (*Green*), CTIP2 (*Orange*) and MAP2 (*Red*). Nuclei counterstained with DAPI (*Blue*). (B) Confocal analysis of parental control iPSC derived neurons co-cultured with mouse astrocytes at 3DIV and fixed at 32DIV in immunostained for PSD-95 or AMPA-R (*Orange*), Synaptophysin (*Red*) and MAP2 (*Green*) Nuclei counterstained with DAPI (*Blue*). (C) High-magnification images from B. The scale bar represents 50µm.

3.2 Synaptic quantification

Antibody based approaches have been extensively used on primary cultures to assess synapses *in vitro* but not in mature iPSC derived neuronal cultures. Furthermore, conventional systems are generally incapable of performing fast batch acquisition of samples and the correspondent image analysis, which limits their use on drug development programs. We then sought to perform synaptic quantification on a high-throughput confocal imaging system. Images of co-cultures immunostained for pre and postsynaptic proteins were acquired by using the high-throughput Opera Phenix confocal microscope and analyzed with a script developed for the Columbus™ image analysis software. The script created a mask around the immunostained neuronal markers which is defined as a search region. In this region, the pre and post synaptic compartments are identified by the immunostaining for synaptophysin and PSD-95 respectively. Then the software calculates the number of puncta and the partial puncta overlappping represented as Pearson's correlation coeficient. To assess if the script could perform synaptic quantification, control iPSC cells were cultured in the presence or absence of growth factors for 17 days. Since MAP2 also co-localized within the mouse astrocytes, a significant percentage of the detected PSD-95 puncta was wrongly identified outside the neurites (Figure 7A) The Pearson's correlation coefficient values were low and no differences were found after growth factors removal (Figure 7B) which could be partially due to the wrong identification of the post-synaptic protein outside the neuronal processes.

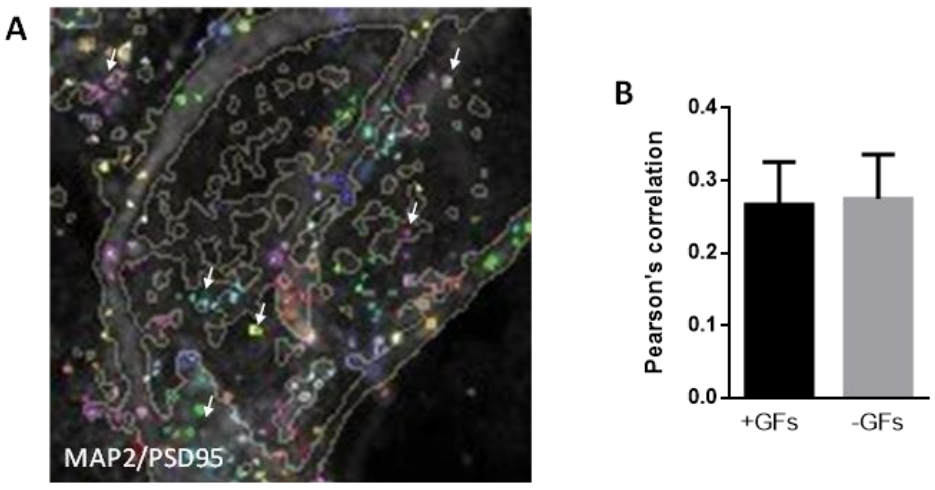

Figure 7. Script analysis quantification with MAP2 immunostaining. (A) Overlay of neurite masks on PSD-95 identified by Columbus script for synaptic quantification. PSD95 identification outside the regions outside the neurites (*white arrows*) (B) Pearson's correlation coefficient of cultures with and without growth factors removed at 13DIV.

In order to have a mask drawn specifically on the neurons we compared immunostained class III beta-tubulin (TUJ1) and human tau protein using DAKO-Tau antibody. Both proteins were detected in neurons and co-stained with the astrocytes with an antibody against glial acidic fibrillary protein (GFAP, Figure 8A and C). We observed that TUJ1 antibody was very specific for the neurons producing less background with low staining of astrocytes which was previously observed with MAP2 immunolabeling (Figure 8B). The anti-human specific Tau antibody (DAKO) was able to detect the presence of the protein on the astrocytes (Figure 8D), which could result in similar synaptic quantification done with MAP2. We then compared the script mask and protein

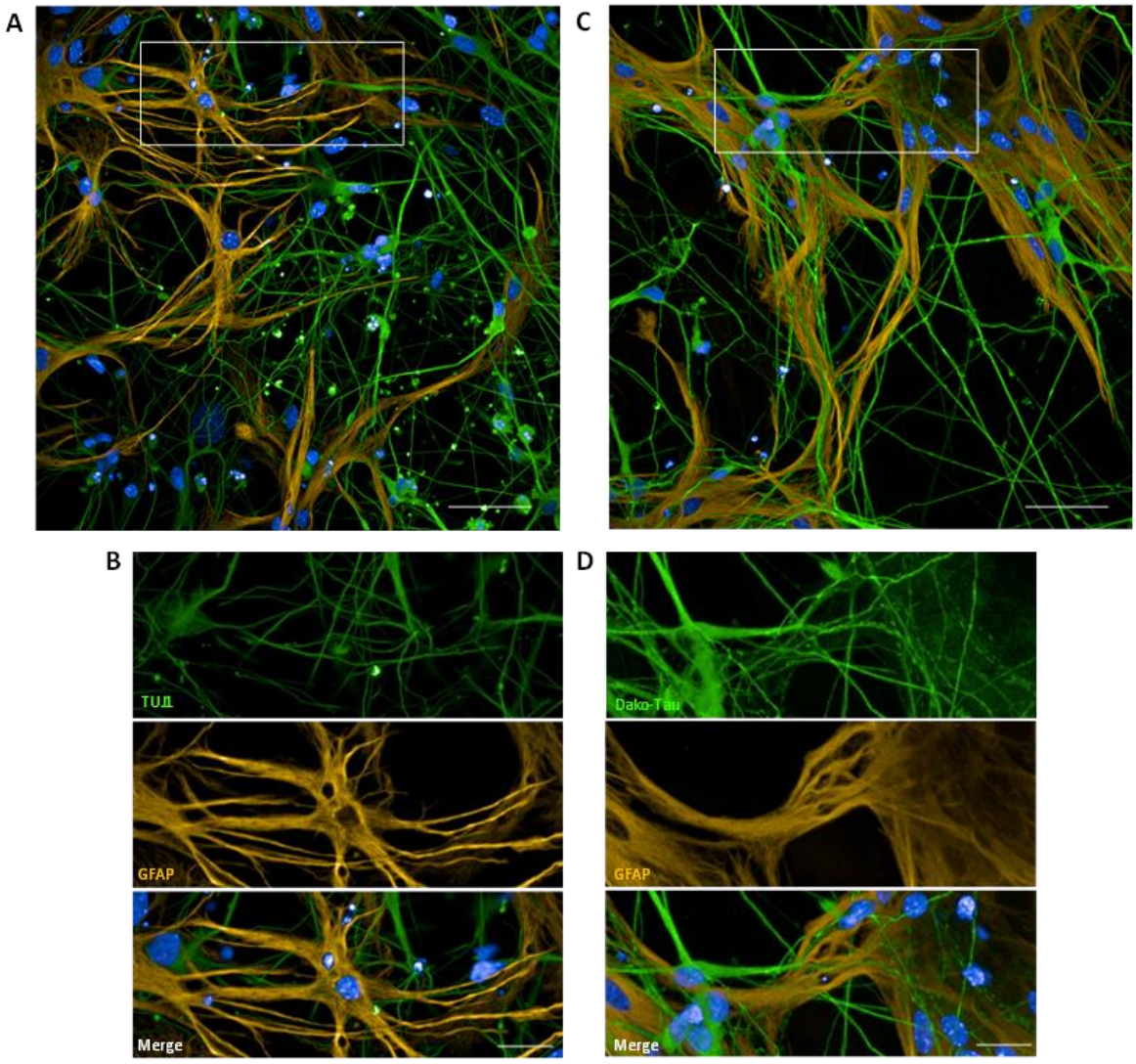

Figure 8. Immunolabeling with TUJ1 antibody results is highly specific for the neurites (A and C) Confocal analysis of parental control iPSC derived neurons co-cultured with mouse astrocytes at 3DIV and fixed at 32-35DIV immunostained for class III β-tubulin using TUJ1 antibody or for anti tau protein using DAKO-Tau antibody (*Green*) and GFAP antibody (*Orange*). Nuclei counterstained with DAPI (*Blue*). (B and D) Immunolabeling of neurons and astrocytes show specificity of neuronal markers class III β-tubulin and MAP2. The scale bar represents 50µm.

identification between TUJ1 and MAP2 immunostained samples co-stained for the postsynaptic protein PSD-95 (Figure 9A and B). Once more, the script did a partial detection of MAP2 in the astrocytes which was not observed when TUJ1 was used (Figure 9 B and D). Moreover, overlay of the TUJ1 mask on the PSD-95 identified by the script clearly shows that the immunolabeled post-synaptic protein was exclusively identified on the neurites contrary to the MAP2 immunolabeling (Figure 10A). This could be used to improve synaptic quantification of co-cultures using the developed script however, the Pearson's correlation coefficient was still low and no differences were found when growth factors were removed from the culture medium. (Figure 10B). Due to antibodies specificity issues, the high background, and lack of robustness we decided to simultaneously develop a reporter-based approach that could provide more reliable results.

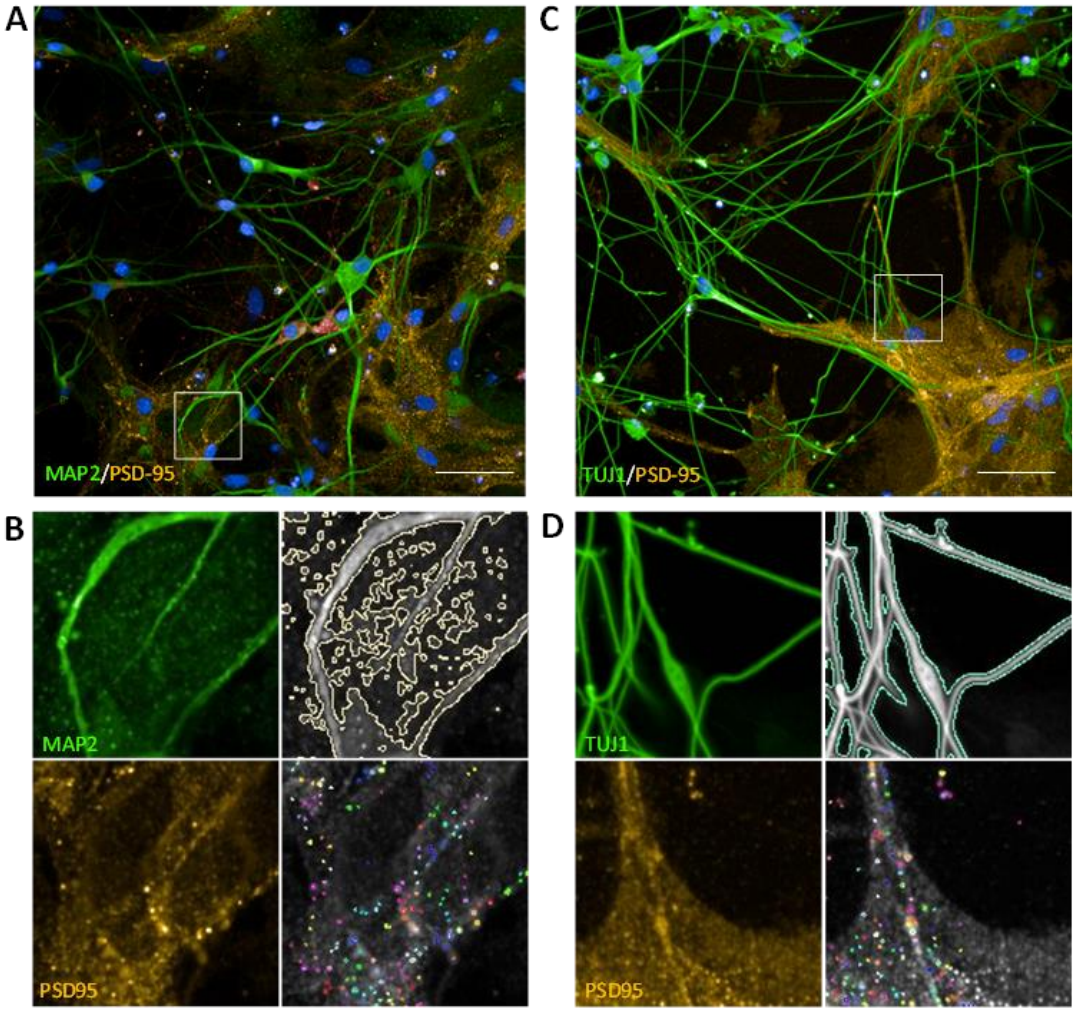

Figure 9. Synaptic quantification using developed script for Columbus software (A and C) Confocal analysis of parental control iPSC derived neurons co-cultured with mouse astrocytes at 33DIV and fixed at DIV62-65 immunostained for MAP2 or for class III β-tubulin using TUJ1 antibody (*Green*) and PSD95 antibody. Nuclei counterstained with DAPI (Blue). The scale bar represents 50µm. (B and D) Script processing of A and C confocal images.

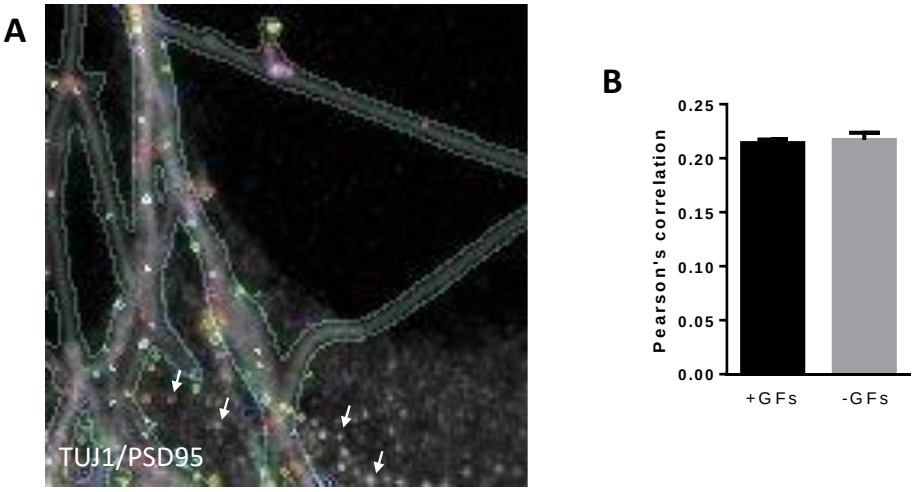

Figure 10. Script analysis quantification with TUJ1 immunostaining. (A) Overlay of neurite masks on PSD-95 identified by Columbus script for synaptic quantification. No identification of PSD-95 outside the neurites (*white arrows*) (B) Pearson's correlation coefficient of cultures with and without growth factors removed at 13DIV.

3.3 Validation of structural and functional reporters in primary and iPSC derived neuronal cultures

Gene reporters have been used to track the location of a protein of interest. The protein can be expressed fused with a fluorescent tag protein which can be detected in different wavelengths. Most of the constructs are composed by a single protein fused with the respective tag and the simultaneously expression of two constructs is usually performed by co-transfection of two of these constructs. More recently, the development of multicistronic genes allowed the expression of two different proteins in the same cell. Here we asked if a dual reporter could be used to detect both pre and post synaptic compartments. The report includes synaptophysin and PSD95 protein sequences fused with GFP and mKate2 tags respectively and are constitutive expressed

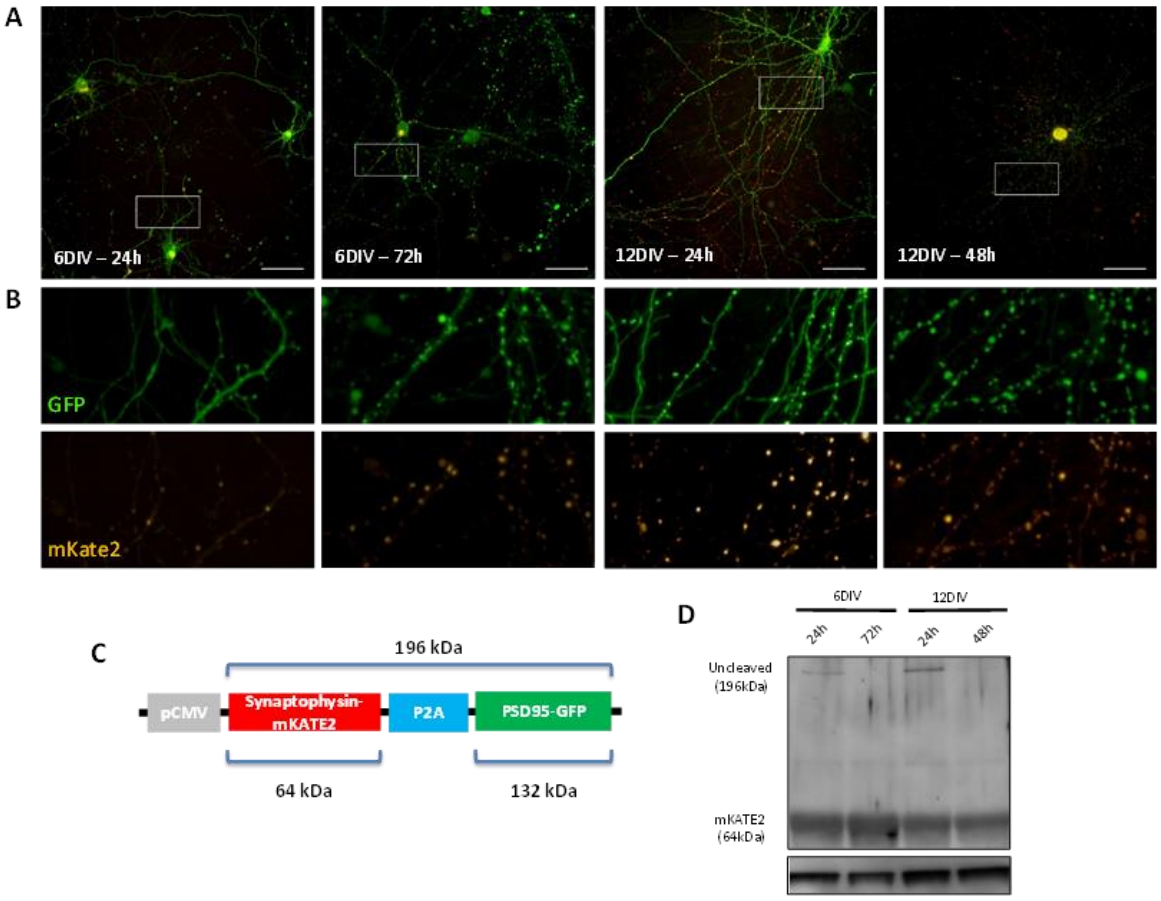

Figure 11. The dual report produces two tagged proteins more efficiently cleaved after 48 to 72 hours (A) Calcium phosphate transfection of primary rat neuronal cultures at 6 or 12DIV fixed 24 to 72 hours after transfection and imaged by confocal imaging in Opera Phenix. (B) High magnification of neurites expressing the two tagged proteins. (C) Representative scheme of the dual reporter weighting 196kDa. Synaptophysin-mKate2 (64kDa) and PSD95-GFP (132kDa). (D) Immunoblot of cell extracts immunostained with an antibody against mKate2.

under a CMV promoter (Figure 11C). We transfected murine cortical neuronal cultures at 6 and 12DIV following a calcium phosphate transient transfection protocol with evaluation of the cleavage efficiency and correct targeting of the construct after 24 and 48 or 72 hours by confocal microscopy and western blot. Immunoblotting of mKate2 tag protein shows the presence of a high molecular weight band corresponding to the uncleaved protein (196kDa) at 24 hours which was absent after 48 and 72 hours, independently of the culture age (Figure 11D). Confocal images show that 12DIV primary cultures network are more developed than at 6DIV and further support the evidence that at 48 or 72 hours the construct is more efficiently cleaved at these timepoints as seen by the presence of a punctated distribution of the construct (Figure 11A and B). To further prove the correct targeting of the construct we performed immunolabeling of a third protein that could identify the synapses such as synapsin, Vglut1 and actin. Transects were drawn over puncta containing the tagged proteins and we observed a perfect match of the profiles at 24 hours suggesting the presence of the uncleaved protein whereas after 48h there was a shift between the two tagged green and red profiles, suggesting a spatial separation of the two constructs (Figure 12). In addition, 48h transfected neurons were immunostained with other antibodies to confirm the correct cleavage and subcellular location of the reporters. Counterstaining with a third component of the synapses allowed us to detect the presence of the single tagged proteins at the synapses. Figure 13 shows how all possible combinations are detected: pre-synaptic reporter with a third marker, post-synaptic reporter with the third marker; and the proteins together. This set of experiments allowed us to conclude that each reporter is correctly tagged to the synapses.

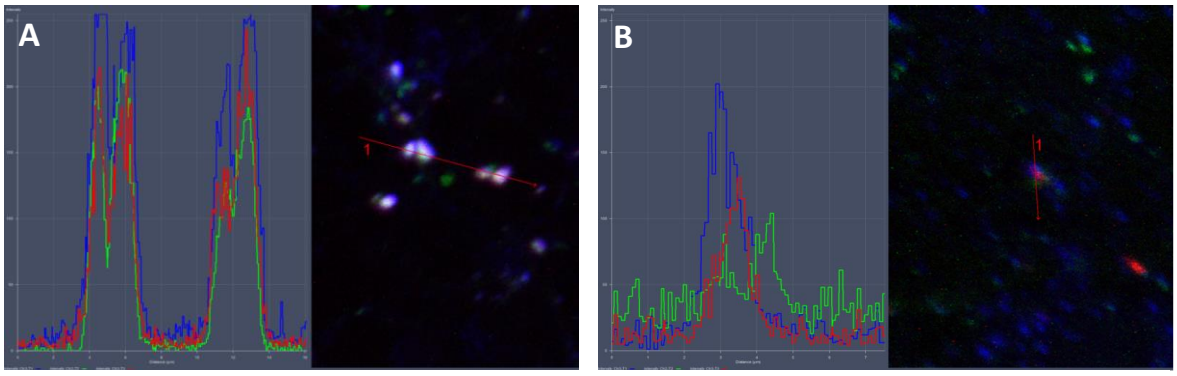

Figure 12. Transects drawn show spatial separation of the constructs over time. Fluorescent intensity profiles of confocal images of primary rat cortical neuronal cultures transfected with the dual reporter at 12DIV. (A) Profiles of fixed cells at 13DIV with synaptophysin immunostaining to compare the profiles of the same protein when detected by its own tag (mKate2) and by a secondary antibody. (B) Profiles of fixed cells at 14DIV with synapsin immunolabeling

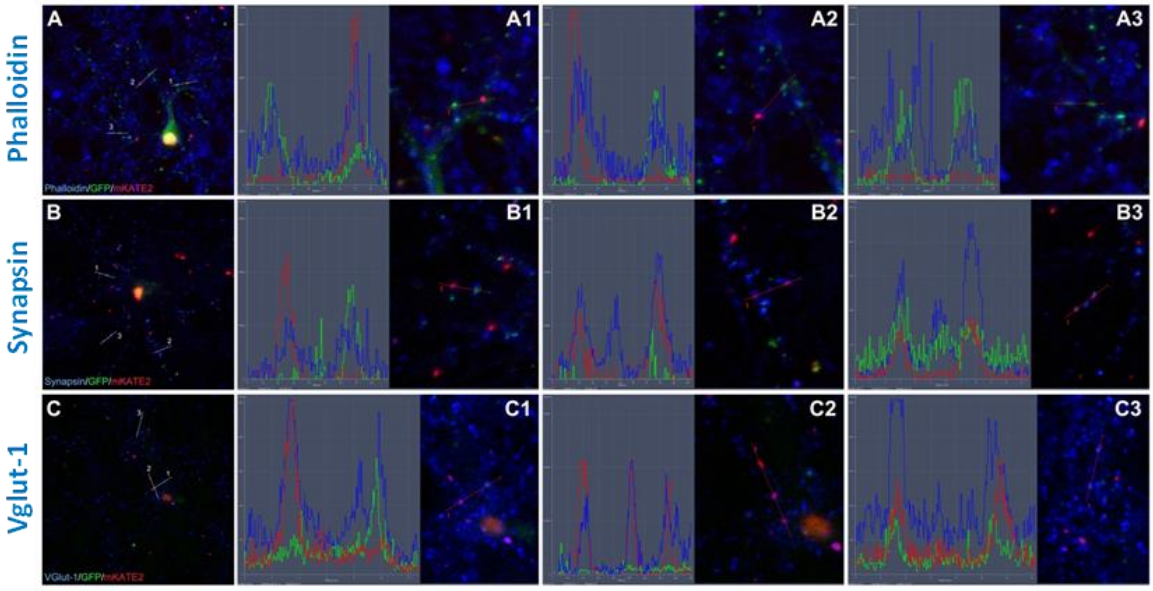

Figure 13. Transects drawn over puncta show all possible combinations. Confocal analysis of primary rat cortical neuronal cultures transfected with the dual reporter at 12DIV and fixed at 15DIV in. Immunostained for actin using Phalloidin conjugated secondary antibody, synapsin and Vglut1 antibody. The profile for PSD95-GFP is shown in green, synaptophysin-mKate2 is shown in red. And the third immunolabeled marker is shown in blue. Three transects were drawn per condition.

3.4 Development of a functional assay to measure electrical activity in cortical neurons *in vitro*

Maturation of neurons results in the creation and strengthening of connections between different cells which is necessary to a correct transmission of information. At the functional level, classical electrophysiology studies based on patch clamp and current clamp approaches have been used to measure electrical activity of primary cultures and to a lesser extent iPSC derived cortical neurons [63,64]. Here, we aimed to record the electrical activity of mature parental control cell line and the double mutant cell line 7H6-A1 iPSC derived neuronal cultures over several weeks plated in Matrigel or PLO-Laminin substrates. We have recorded the electrical activity using microelectrode array plates (MEAs) and analyzed the number of spikes, number of bursts and mean firing rate. The control cell line shows an increase in the spike numbers which starts to decrease from DIV 34 whereas the double mutant cell line shows a steady increase with small increase after DIV 36 suggesting it may be reaching a plateau of activity (Figure 14A). Furthermore, in the double mutant cell line cultures nearly all electrodes were activated compared to the activation of 65% of the total number of electrodes in the control cells (Figure 14B). Different parameters were plotted comparing the two cell lines platted in different substrates in cultures with 34DIV. Both number of

spikes, number of bursts and mean firing were always higher in the mutant cell line independently of the use of Matrigel or laminin as substrates (Figure 14C).

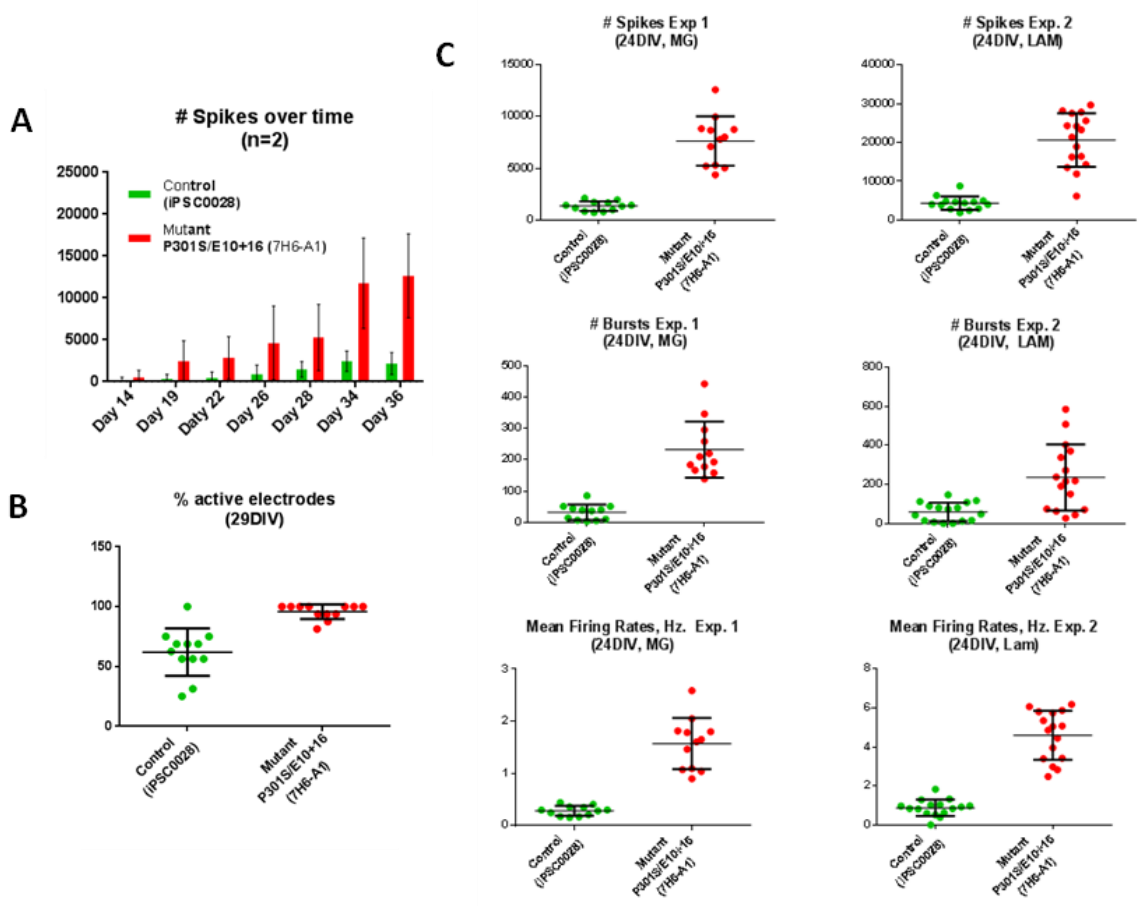

Figure 14. NPC double mutant cell line 7H6-A1 is more active than NPC control cell line. All experiments were performed with comparison between control and double mutant cell line. (A) Time course analysis of number of spikes (two independent experiments) (B) summary plot of the percentage of active electrodes of 29DIV cultures (C) summary plot of the number of spikes, number of bursts and mean firing rates of 24DIV cultures plated on matrigel (Exp. 1) or laminin (Exp. 2) substrates.

4 Discussion

4.1 Synaptic quantification using antibodies

In this study we show that is possible to do synaptic quantification of iPSC derived neurons co-cultured with astrocytes using an antibody based approach and analyzed by an automated script. The MAP2 immunoreactivity observed in astrocytes is consistent with previous studies where tau protein was shown to be present in the astrocytes in the brains of patients with progressive supranuclear palsy, corticobasal degeneration and Pick's disease [65,66] . Furthermore, an algorithm based on the transcriptome of different cell types present in the cortex show that astrocytes may also express this protein. This suggest that MAP2 may not suitable to stain iPSC derived neurons co-cultures with astrocytes since the script will also create a mask inside the astrocytes and contribute to detection of PSD95 puncta from these cells. Astrocytes may also mediate phagocytic elimination of neuronal synapses which may explain the presence of the postsynaptic protein PSD95[67]. With the validation of the TUJ1 antibody against class III beta tubulin, the script is now able to do a more precise identification of the synaptic proteins belonging to neurites. Nevertheless, this approach still presents a challenge mainly due to cell culture conditions, antibodies variability and low robustness between assays.

4.2 Synaptic quantification with reporters

To improve identification of synapses, we show that a dual reporter could present some advantages over the antibodies. The captures with the single construct PSD95-GFP are similar to the ones obtained in previous studies[68]. The two proteins in the dual reporter are separated by a self-cleaving p2A peptide which has been used in bicistronic reporters on murine neurons[69]. During protein translation, the ribosomes skip the translation of this peptide, jumping to the translation of the second protein located downstream[70]. We expected an increase in the single tagged protein after cleavage of the p2A peptide which was not observed. One explanation could be the presence of control mechanisms that helps eliminating the newly synthetized protein. Overall our results suggest that the dual reporter is successfully cleaved and it produces two separated proteins which seem to be targeted to cluster like structures along the neurites. However, with the imaging resolution available we cannot guarantee that the proteins are being targeted to synapses. Moreover, since both constructs are under CMV constitutive expression it may impair the cellular health and numerous intracellular processes which may include the correct targeting and anchorage of the synaptic proteins in synapses. To allow a less stressful expression of the construct, we will be testing the same reporter under an inducible promoter

such as doxycycline to reduce the amount of excessive protein that is produced during constitutive expression. In a later stage it could be introduced into a viral vector to allow a greater transfection rate, which could allow us to study the synaptic connections between neighbour neurons *in vitro* and *in vivo*.

4.3 Neuronal electrical activity

In this study we show that the double mutant cell line presents consistent higher neuronal activity than the control cell line independently of the platting substrate. However, optimal recording conditions in iPSC derived neuronal cultures have not been yet optimized. The neuronal culture media could be impairing neuronal activity as it is only know to promote cell survival but the functional consequences are not well elucidated. In a previous study serum and supplements included in the media have been shown to impair the generation of action potentials. The use of a serum-free media as BrainPhys was able to promote the neuronal electrical activity which was translated into a higher number of active electrodes and electrical activity recorded[71]. Multielectrode arrays have shown hyperactivity of iPSC derived motor neurons from ALS individuals[72] however little data exists on Alzheimer's disease iPSC derived neuronal cultures. We still have to elucidate if the differences found between control and mutant cell lines are due to the isogenic or the P301S mutation. Therefore we are currently comparing the control and double mutant cell lines with a single mutant expressing the isogenic mutation together with overexpression of P301S mutated tau gene on control cells or knockdown of the 4R tau isoforms to better understand the neuronal activity of these cell lines.

5 References

1. Reitz, C.; Mayeux, R. Alzheimer Disease: Epidemiology, Diagnostic Criteria, Risk Factors and Biomarkers. *Biochem. Pharmacol.* **2014**, *88*, 640–651.

2. Karran, E.; Mercken, M.; De Strooper, B. The Amyloid Cascade Hypothesis for Alzheimer's Disease: An Appraisal for the Development of Therapeutics. *Nat. Rev. Drug Discov.* **2011**, *10*, 698–712.

3. Glenner, G. G.; Wong, C. W. Alzheimer's Disease: Initial Report of the Purification and Characterization of a Novel Cerebrovascular Amyloid Protein. *Biochem. Biophys. Res. Commun.* **1984**, *120*, 885–890.

4. Haass, C.; Selkoe, D. J. Cellular Processing of Beta-Amyloid Precursor Protein and the Genesis of Amyloid Beta-Peptide. *Cell* **1993**, *75*, 1039–1042.

5. Kojro, E.; Fahrenholz, F. The Non-Amyloidogenic Pathway: Structure and Function of Alpha-Secretases. *Subcell. Biochem.* **2005**, *38*, 105–27.

6. Jarrett, J. T.; Berger, E. P.; Lansbury, P. T. The Carboxy Terminus of the Beta Amyloid Protein Is Critical for the Seeding of Amyloid Formation: Implications for the Pathogenesis of Alzheimer's Disease. *Biochemistry* **1993**, *32*, 4693–4697.

7. LaFerla, F. M.; Green, K. N.; Oddo, S. Intracellular Amyloid-β in Alzheimer's Disease. *Nat. Rev. Neurosci.* **2007**, *8*, 499–509.

8. Binder, L. I.; Frankfurter, A.; Rebhun, L. I. Differential Localization of MAP-2 and Tau in Mammalian Neurons in Situ. *Ann N Y Acad Sci* **1986**, *466*, 145–166.

9. Sergeant, N.; Delacourte, A.; Buée, L. Tau Protein as a Differential Biomarker of Tauopathies. *Biochim. Biophys. Acta - Mol. Basis Dis.* **2005**, *1739*, 179–197.

10. Barghorn, S.; Mandelkow, E. Toward a Unified Scheme for the Aggregation of Tau into Alzheimer Paired Helical Filaments. *Biochemistry* **2002**, *41*, 14885–14896.

11. Wang, Y.; Mandelkow, E. Tau in Physiology and Pathology. *Nat Rev Neurosci* **2016**, *17*, 5–21.

12. Sergeant, N.; Bretteville, A.; Hamdane, M.; et al. Biochemistry of Tau in Alzheimer's Disease and Related Neurological Disorders. *Expert Rev. Proteomics* **2008**, *5*, 207–224.

13. Hanger, D. P.; Hughes, K.; Woodgett, J. R.; et al. Glycogen Synthase Kinase-3 Induces Alzheimer's Disease-like Phosphorylation of Tau: Generation of Paired Helical Filament Epitopes and Neuronal Localisation of the Kinase. *Neurosci. Lett.* **1992**, *147*, 58–62.

14. Mandelkow, E. M.; Drewes, G.; Biernat, J.; et al. Glycogen Synthase Kinase-3 and the Alzheimer-like State of Microtubule-Associated Protein Tau. *FEBS Lett.* **1992**, *314*, 315–321.

15. Rankin, C. a; Sun, Q.; Gamblin, T. C. Tau Phosphorylation by GSK-3beta Promotes Tangle-like Filament Morphology. *Mol. Neurodegener.* **2007**, *2*, 12.

16. Grundke-Iqbal, I.; Iqbal, K.; Tung, Y. C.; et al. Abnormal Phosphorylation of the Microtubule-Associated Protein Tau (Tau) in Alzheimer Cytoskeletal Pathology. *Proc. Natl. Acad. Sci. U. S. A.* **1986**, *83*, 4913–7.

17. Ihara, Y.; Nukina, N.; Miura, R.; et al. Phosphorylated Tau Protein Is Integrated into Paired Helical Filaments in Alzheimer's Disease. *J. Biochem.* **1986**, *99*, 1807–1810.

18. Kosik, K. S.; Joachim, C. L.; Selkoe, D. J. Microtubule-Associated Protein Tau (Tau) Is a Major Antigenic Component of Paired Helical Filaments in Alzheimer Disease. *Proc. Natl. Acad. Sci. U. S. A.* **1986**, *83*, 4044–4048.

19. Martin, L.; Latypova, X.; Terro, F. Post-Translational Modifications of Tau Protein: Implications for Alzheimer's Disease. *Neurochem. Int.* **2011**, *58*, 458–471.

20. Derisbourg, M.; Leghay, C.; Chiappetta, G.; et al. Role of the Tau N-Terminal Region in Microtubule Stabilization Revealed by New Endogenous Truncated Forms. *Sci. Rep.* **2015**, *5*, 9659.

21. Flores-Rodríguez, P.; Ontiveros-Torres, M. A.; Cárdenas-Aguayo, M. C.; et al. The Relationship between Truncation and Phosphorylation at the C-Terminus of Tau Protein in the Paired Helical Filaments of Alzheimer's Disease. *Front. Neurosci.* **2015**, *9*, 33.

22. Gamblin, T. C.; Chen, F.; Zambrano, A.; et al. Caspase Cleavage of Tau: Linking Amyloid and Neurofibrillary Tangles in Alzheimer's Disease. *Proc. Natl. Acad. Sci. U. S. A.* **2003**, *100*, 10032–10037.

23. Selkoe, D. J. Alzheimer's Disease: Genes, Proteins, and Therapy. *Physiol. Rev.* **2001**, *81*, 741–66.

24. De Strooper, B.; Vassar, R.; Golde, T. The Secretases: Enzymes with Therapeutic Potential in Alzheimer Disease. *Nat. Rev. Neurol.* **2010**, *6*, 99–107.

25. Liu, C.-C.; Kanekiyo, T.; Xu, H.; et al. Apolipoprotein E and Alzheimer Disease: Risk, Mechanisms and Therapy. *Nat Rev Neurol* **2013**, *9*, 106–118.

26. Zhong, N.; Ramaswamy, G.; Weisgraber, K. H. Apolipoprotein E4 Domain Interaction Induces Endoplasmic Reticulum Stress and Impairs Astrocyte Function. *J. Biol. Chem.* **2009**, *284*, 27273–27280.

27. Holtzman, D. M.; Bales, K. R.; Tenkova, T.; et al. Apolipoprotein E Isoform-Dependent Amyloid Deposition and Neuritic Degeneration in a Mouse Model of Alzheimer's Disease. *Proc. Natl. Acad. Sci. U. S. A.* **2000**, *97*, 2892–7.

28. Schmechel, D. E.; Saunders, A. M.; Strittmatter, W. J.; et al. Increased Amyloid Beta-Peptide Deposition in Cerebral Cortex as a Consequence of Apolipoprotein E Genotype in Late-Onset Alzheimer Disease. *Proc. Natl. Acad. Sci. U. S. A.* **1993**, *90*, 9649–53.

29. Strittmatter, W. J.; Saunders, A. M.; Schmechel, D.; et al. Apolipoprotein E: High-Avidity Binding to B-Amyloid and Increased Frequency of Type 4 Allele in Late-Onset Familial Alzheimer Disease. *Proc. Natl. Acad. Sci. U. S. A.* **1993**, *90*, 1977–1981.

30. Zheng, W. H.; Bastianetto, S.; Mennicken, F.; et al. Amyloid Beta Peptide Induces Tau Phosphorylation and Loss of Cholinergic Neurons in Rat Primary Septal Cultures. *Neuroscience* **2002**, *115*, 201–211.

31. Gustafson, D. R.; Skoog, I.; Rosengren, L.; et al. Cerebrospinal Fluid Beta-Amyloid 1-

42 Concentration May Predict Cognitive Decline in Older Women. *J. Neurol. Neurosurg. Psychiatry* **2007**, *78*, 461–4.

32. Jack Jr., C. R.; Wiste, H. J.; Weigand, S. D.; et al. Amyloid-First and Neurodegeneration-First Profiles Characterize Incident Amyloid PET Positivity. *Neurology* **2013**, *81*, 1732–1740.

33. Braak, H.; Del Tredici, K. Where, When, and in What Form Does Sporadic Alzheimer's Disease Begin? *Curr Opin Neurol* **2012**, *25*, 708–714.

34. Hurtado, D. E.; Molina-Porcel, L.; Iba, M.; et al. A{beta} Accelerates the Spatiotemporal Progression of Tau Pathology and Augments Tau Amyloidosis in an Alzheimer Mouse Model. *Am J Pathol* **2010**, *177*, 1977–1988.

35. Walker, L. C.; Diamond, M. I.; Duff, K. E.; et al. Mechanisms of Protein Seeding in Neurodegenerative Diseases. *JAMA Neurol* **2013**, *70*, 304–310.

36. Guo, J. L.; Lee, V. M. Seeding of Normal Tau by Pathological Tau Conformers Drives Pathogenesis of Alzheimer-like Tangles. *J Biol Chem* **2011**, *286*, 15317–15331.

37. Ittner, L. M.; Götz, J. Amyloid-β and Tau — a Toxic Pas de Deux in Alzheimer's Disease. *Nat. Rev. Neurosci.* **2011**, *12*, 65–72.

38. Mazzaro, N.; Barini, E.; Spillantini, M. G.; et al. Tau-Driven Neuronal and Neurotrophic Dysfunction in a Mouse Model of Early Tauopathy. *J. Neurosci.* **2016**, *36*, 2086–2100.

39. De Felice, F. G.; Velasco, P. T.; Lambert, M. P.; et al. Abeta Oligomers Induce Neuronal Oxidative Stress through an N-Methyl-D-Aspartate Receptor-Dependent Mechanism That Is Blocked by the Alzheimer Drug Memantine. *J. Biol. Chem.* **2007**, *282*, 11590–11601.

40. Spires-Jones, T. L.; Hyman, B. T. The Intersection of Amyloid Beta and Tau at Synapses in Alzheimer's Disease. *Neuron* **2014**, *82*, 756–771.

41. Vossel, K. A.; Xu, J. C.; Fomenko, V.; et al. Tau Reduction Prevents Aβ-Induced Axonal Transport Deficits by Blocking Activation of GSK3β. *J. Cell Biol.* **2015**, *209*, 419–433.

42. Sokolow, S.; Henkins, K. M.; Bilousova, T.; et al. Pre-Synaptic C-Terminal Truncated Tau Is Released from Cortical Synapses in Alzheimer's Disease. *J. Neurochem.* **2015**, *133*, 368–379.

43. DeKosky, S. T.; Scheff, S. W. Synapse Loss in Frontal Cortex Biopsies in Alzheimer's Disease: Correlation with Cognitive Severity. *Ann. Neurol.* **1990**, *27*, 457–464.

44. Scheff, S. W.; Price, D. A.; Schmitt, F. A.; et al. Synaptic Loss in the Inferior Temporal Gyrus in Mild Cognitive Impairment and Alzheimer's Disease. *J. Alzheimers. Dis.* **2011**, *24*, 547–557.

45. Terry, R. D.; Masliah, E.; Salmon, D. P.; et al. Physical Basis of Cognitive Alterations in Alzheimer's Disease: Synapse Loss Is the Major Correlate of Cognitive Impairment. *Ann. Neurol.* **1991**, *30*, 572–580.

46. Scheff, S. W.; Price, D. A.; Ansari, M. A.; et al. Synaptic Change in the Posterior

Cingulate Gyrus in the Progression of Alzheimer's Disease. *J. Alzheimer's Dis.* **2015**, *43*, 1073–1090.

47. Evans, M. J.; Kaufman, M. H. Establishment in Culture of Pluripotential Cells from Mouse Embryos. *Nature*, 1981, *292*, 154–156.

48. Takahashi, K.; Tanabe, K.; Ohnuki, M.; et al. Induction of Pluripotent Stem Cells from Adult Human Fibroblasts by Defined Factors. *Cell* **2007**, *131*, 861–872.

49. Avior, Y.; Sagi, I.; Benvenisty, N. Pluripotent Stem Cells in Disease Modelling and Drug Discovery. *Nat Rev Mol Cell Biol* **2016**, *17*, 170–182.

50. Israel, M. A.; Yuan, S. H.; Bardy, C.; et al. Probing Sporadic and Familial Alzheimer's Disease Using Induced Pluripotent Stem Cells. *Nature* **2012**, *482*, 216–20.

51. Kondo, T.; Asai, M.; Tsukita, K.; et al. Modeling Alzheimer's Disease with iPSCs Reveals Stress Phenotypes Associated with Intracellular A?? And Differential Drug Responsiveness. *Cell Stem Cell* **2013**, *12*, 487–496.

52. Muratore, C. R.; Rice, H. C.; Srikanth, P.; et al. The Familial Alzheimer's Disease APPV717I Mutation Alters APP Processing and Tau Expression in iPSC-Derived Neurons. *Hum. Mol. Genet.* **2014**, *23*, 3523–3536.

53. Yagi, T.; Ito, D.; Okada, Y.; et al. Modeling Familial Alzheimer's Disease with Induced Pluripotent Stem Cells. *Hum. Mol. Genet.* **2011**, *20*, 4530–4539.

54. Sproul, A. A.; Jacob, S.; Pre, D.; et al. Characterization and Molecular Profiling of PSEN1 Familial Alzheimer's Disease iPSC-Derived Neural Progenitors. *PLoS One* **2014**, *9*.

55. Moore, S.; Evans, L. D. B.; Andersson, T.; et al. APP Metabolism Regulates Tau Proteostasis in Human Cerebral Cortex Neurons. *Cell Rep.* **2015**, *11*, 689–696.

56. Choi, S. H.; Kim, Y. H.; Hebisch, M.; et al. A Three-Dimensional Human Neural Cell Culture Model of Alzheimer's Disease. *Nature* **2014**, *515*, 274–8.

57. Iovino, M.; Agathou, S.; Gonzalez-Rueda, A.; et al. Early Maturation and Distinct Tau Pathology in Induced Pluripotent Stem Cell-Derived Neurons from Patients with MAPT Mutations. *Brain* **2015**.

58. Schoch, K. M.; DeVos, S. L.; Miller, R. L.; et al. Increased 4R-Tau Induces Pathological Changes in a Human-Tau Mouse Model. *Neuron* **2016**, *90*, 941–947.

59. Orr, D. J.; Smith, R. A. Neuronal Maintenance and Neurite Extension of Adult Mouse Neurones in Non-Neuronal Cell-Reduced Cultures Is Dependent on Substratum Coating. *J Cell Sci* **1988**, *91 (Pt 4)*, 555–561.

60. Shi, Y.; Kirwan, P.; Smith, J.; et al. Human Cerebral Cortex Development from Pluripotent Stem Cells to Functional Excitatory Synapses. *Nat Neurosci* **2012**, *15*, 477–86, S1.

61. Theocharatos, S.; Wilkinson, D. J.; Darling, S.; et al. Regulation of Progenitor Cell Proliferation and Neuronal Differentiation in Enteric Nervous System Neurospheres. *PLoS One* **2013**, *8*, e54809.

62. Kaech, S.; Banker, G. Culturing Hippocampal Neurons. *Nat. Protoc.* **2006**, *1*, 2406–

15.

63. Belinsky, G. S.; Rich, M. T.; Sirois, C. L.; et al. Patch-Clamp Recordings and Calcium Imaging Followed by Single-Cell PCR Reveal the Developmental Profile of 13 Genes in iPSC-Derived Human Neurons. *Stem Cell Res.* **2014**, *12*, 101–118.

64. Maximov, A.; Pang, Z. P.; Tervo, D. G.; et al. Monitoring Synaptic Transmission in Primary Neuronal Cultures Using Local Extracellular Stimulation. *J Neurosci Methods* **2007**, *161*, 75–87.

65. Komori, T. Tau-Positive Glial Inclusions in Progressive Supranuclear Palsy, Corticobasal Degeneration and Pick's Disease. *Brain Pathol.* **1999**, *9*, 663–79.

66. Togo, T.; Dickson, D. W. Tau Accumulation in Astrocytes in Progressive Supranuclear Palsy Is a Degenerative rather than a Reactive Process. *Acta Neuropathol.* **2002**, *104*, 398–402.

67. Chung, W.-S.; Clarke, L. E.; Wang, G. X.; et al. Astrocytes Mediate Synapse Elimination through MEGF10 and MERTK Pathways. *Nature* **2013**, *504*, 394–400.

68. Marrs, G. S.; Green, S. H.; Dailey, M. E. Rapid Formation and Remodeling of Postsynaptic Densities in Developing Dendrites. *Nat. Neurosci.* **2001**, *4*, 1006–13.

69. Tang, W.; Ehrlich, I.; Wolff, S. B.; et al. Faithful Expression of Multiple Proteins via 2A-Peptide Self-Processing: A Versatile and Reliable Method for Manipulating Brain Circuits. *J Neurosci* **2009**, *29*, 8621–8629.

70. Donnelly, M. L.; Luke, G.; Mehrotra, A.; et al. Analysis of the Aphthovirus 2A/2B Polyprotein "Cleavage" Mechanism Indicates Not a Proteolytic Reaction, but a Novel Translational Effect: A Putative Ribosomal "Skip." *J Gen Virol* **2001**, *82*, 1013–1025.

71. Bardy, C.; van den Hurk, M.; Eames, T.; et al. Neuronal Medium That Supports Basic Synaptic Functions and Activity of Human Neurons in Vitro. *Proc Natl Acad Sci U S A* **2015**, *112*, E2725–34.

72. Wainger, B. J.; Kiskinis, E.; Mellin, C.; et al. Intrinsic Membrane Hyperexcitability of Amyotrophic Lateral Sclerosis Patient-Derived Motor Neurons. *Cell Rep.* **2014**, *7*, 1–11.